

Central Lancashire Online Knowledge (CLoK)

Title	Investigating the role of CD44 and hyaluronate in embryo-epithelial interaction using an in vitro model
Type	Article
URL	https://clock.uclan.ac.uk/31549/
DOI	##doi##
Date	2019
Citation	Berneau, Stephane orcid iconORCID: 0000-0003-4181-2745, Ruane, P.T., Brison, D.R., Kimber, S.J., Westwood, M. and Aplin, J.D. (2019) Investigating the role of CD44 and hyaluronate in embryo-epithelial interaction using an in vitro model. <i>Molecular Human Reproduction</i> , 25 (5). pp. 265-273. ISSN 1360-9947
Creators	Berneau, Stephane, Ruane, P.T., Brison, D.R., Kimber, S.J., Westwood, M. and Aplin, J.D.

It is advisable to refer to the publisher's version if you intend to cite from the work. ##doi##

For information about Research at UCLan please go to <http://www.uclan.ac.uk/research/>

All outputs in CLoK are protected by Intellectual Property Rights law, including Copyright law. Copyright, IPR and Moral Rights for the works on this site are retained by the individual authors and/or other copyright owners. Terms and conditions for use of this material are defined in the <http://clock.uclan.ac.uk/policies/>



Investigating the role of CD44 and hyaluronate in embryo-epithelial interaction using an in-vitro model

DOI:
[10.1093/molehr/gaz011](https://doi.org/10.1093/molehr/gaz011)

Document Version
Accepted author manuscript

[Link to publication record in Manchester Research Explorer](#)

Citation for published version (APA):
Berneau, S., Ruane, P., Brison, D. R., Kimber, S., Westwood, M., & Aplin, J. (2019). Investigating the role of CD44 and hyaluronate in embryo-epithelial interaction using an in-vitro model. *Molecular Human Reproduction*.
<https://doi.org/10.1093/molehr/gaz011>

Published in:
Molecular Human Reproduction

Citing this paper
Please note that where the full-text provided on Manchester Research Explorer is the Author Accepted Manuscript or Proof version this may differ from the final Published version. If citing, it is advised that you check and use the publisher's definitive version.

General rights
Copyright and moral rights for the publications made accessible in the Research Explorer are retained by the authors and/or other copyright owners and it is a condition of accessing publications that users recognise and abide by the legal requirements associated with these rights.

Takedown policy
If you believe that this document breaches copyright please refer to the University of Manchester's Takedown Procedures [<http://man.ac.uk/04Y6Bo>] or contact uml.scholarlycommunications@manchester.ac.uk providing relevant details, so we can investigate your claim.



1 **Investigating the role of CD44 and hyaluronate in embryo-epithelial interaction**
2 **using an in-vitro model**

3 Berneau SC¹, Ruane PT¹, Brison DR^{1,2}, Kimber SJ³, Westwood M¹, Aplin JD¹

4 ¹Maternal and Fetal Health Centre and Division of Developmental Biology and
5 Medicine, Faculty of Biology, Medicine and Health, University of Manchester,
6 Manchester Academic Health Sciences Centre, St Mary's Hospital, Manchester M13
7 9WL, UK

8 ²Department of Reproductive Medicine, Old St Mary's Hospital, Central Manchester
9 University Hospitals NHS Foundation Trust, Manchester Academic Health Science
10 Centre, Oxford Road, Manchester M13 9WL, UK.

11 ³Division of Cell Matrix Biology and Regenerative Medicine, School of Biological
12 Sciences, Faculty of Biology Medicine and Health, University of Manchester, Michael
13 Smith Building, Manchester M13 9PT, UK.

14 **Running title:** CD44 – hyaluronate interaction at implantation

15

16

17

18

19

20

21 **Abstract**

22 Implantation failure is an important impediment to increasing success rates in assisted
23 reproductive technologies (ART). Knowledge of the cascade of morphological and
24 molecular events at implantation remains limited. Cell surface CD44 and hyaluronate
25 (HA) have been reported in the uterus, but a role in intercellular interaction at
26 implantation remains to be evaluated. Mouse embryos were co-cultured with human
27 Ishikawa endometrial epithelial monolayers over two days. Attachment was tenuous
28 during the first 24 hrs, after which it became stable, leading to breaching of the
29 monolayer. The effects of enzymatically reducing the density of HA, or introducing a
30 function-blocking antibody to CD44, were monitored during progression from weak to
31 stable embryonic attachment. Hyaluronidase-mediated removal of surface HA from the
32 epithelial cells enhanced the speed of attachment, while a similar treatment of
33 embryos had no effect. The antibody to CD44 caused retardation of initial attachment.
34 These results suggest that CD44-HA binding could be employed by embryos during
35 initial docking, but the persistence of HA in epithelial cells might be detrimental to later
36 stages of implantation by retarding attainment of stable attachment.

37 **Keywords:** CD44, hyaluronate, implantation, endometrium, embryo adhesion.

38 **Introduction**

39 CD44 is a cell surface glycoprotein that acts as a receptor for hyaluronan (HA) as well
40 as other ligands including osteopontin (OPN), collagens and matrix metalloproteinase
41 9 (Misra *et al.*, 2015, Senbanjo and Chellaiah, 2017). CD44 is present in a wide range
42 of cells, with a complex pattern of splice variants and glycoforms, including the
43 trophoctoderm of both human and mouse blastocysts (Campbell *et al.*, 1995, Lu *et al.*,
44 2002) and endometrial tissue. In the mid secretory phase, when embryo implantation

45 occurs, CD44 is found at the lateral and apical surface of both glandular and luminal
46 epithelial cells (Afify *et al.*, 2006, Albers *et al.*, 1995, Behzad *et al.*, 1994, Fujita *et al.*,
47 1994, Griffith *et al.*, 2010, Saegusa *et al.*, 1998, Saegusa and Okayasu, 1998). Ligand
48 binding to CD44 leads to changes in cell motility, gene expression and growth
49 (Senbanjo and Chellaiah, 2017). The fucosyl transferase FUT4 catalyses the addition
50 of terminal α 1.3-fucosyl residues to glycan on CD44, leading in turn to activation of the
51 Wnt/ β -catenin signalling pathway (Zheng *et al.*, 2017), which is associated with
52 endometrial receptivity to implantation (Mohamed *et al.*, 2005), though an upstream
53 ligand sensitive to glycoform has not been identified.

54 HA is present in uterine fluid and on the surface of the endometrial epithelium
55 (Fouladi-Nashta *et al.*, 2017). Treatment of mouse embryos with HA promoted
56 implantation (Gardner *et al.*, 1999), and HA-containing embryo transfer medium used
57 in ART has been reported to improve implantation and increase live birth rates in
58 humans (Bontekoe *et al.*, 2014). CD44-HA interactions have therefore been implicated
59 in embryo attachment during the early stages of implantation. HA is proposed to bridge
60 between embryo and endometrial epithelium through CD44 (and possibly other
61 receptors), while OPN dimers (Goldsmith *et al.*, 2002) may bridge CD44 and/or integrin
62 α v β 3. OPN is a strong candidate adhesion molecule for implantation (Johnson *et al.*,
63 2014) and we have previously shown that integrin α v β 3-OPN interactions contribute to
64 embryo attachment to epithelium in vitro (Kang *et al.*, 2014). Recent experimental
65 manipulation of HA in the sheep uterus however suggests that endometrial HA may act
66 to inhibit implantation (Fouladi-Nashta *et al.*, 2017, Marei *et al.*, 2017).

67 We have used Ishikawa cells as a model endometrial epithelium for examining
68 interaction with blastocyst stage embryos (Ruane *et al.*, 2017, Ruane *et al.*, 2018,

69 Singh *et al.*, 2010). When embryos are transferred to confluent Ishikawa cell
70 monolayers, initial attachment to the apical surface is followed by breaching and
71 trophoblast outgrowth. A proteomic profile of glycoproteins exposed at the apical
72 surface of confluent, polarised Ishikawa cells included CD44 (Aplin and Ruane, 2017,
73 Singh and Aplin, 2015, Singh *et al.*, 2010), verifying that these cells are suitable for
74 evaluating its biological activity in this context. Here we examine the effects of blocking
75 CD44 as well as stripping cell surface HA on attachment of mouse embryos.

76 **Materials and Methods**

77 *Cell culture*

78 Ishikawa cells (ECACC 99040201) were maintained at 37°C, 95% air and 5% CO₂ in
79 DMEM (Sigma) containing 10% fetal bovine serum (Sigma), 2mM L-glutamine,
80 100µg/ml streptomycin and 100IU/ml penicillin (Sigma). Cells were grown on 2%
81 Matrigel-coated 13mm glass coverslips (Sigma) in 24-well plates (Corning) up to
82 passage 25.

83 *Mouse embryos*

84 Experiments were carried out under UK Home Office project license PPL 70/07838,
85 and authorised by the Animal Welfare and Ethical Review Board of the University of
86 Manchester, according to the Animal Act, 1986. Eight-week-old CD1 female mice
87 (Charles River) were superovulated (by intraperitoneal injection of 5 IU pregnant
88 mare serum gonadotrophin (Intervet), followed by 5 IU human chorionic
89 gonadotrophin (Intervet) 46 hrs later) and time-mated. The 2-cell embryos were
90 flushed from the oviduct at E (embryo day) 1.5. Embryos were cultured in KSOM
91 medium (Millipore) containing 0.4% BSA (Sigma) under oil (Vitrolife) to E4.5 then

92 artificially hatched from the zona pellucidae using acid Tyrode's solution (pH 2.5)
93 (Sigma).

94 *Cell spreading assay*

95 Flat-bottom 48-well plates (Corning) were left uncoated or coated overnight with
96 5µg/ml osteopontin (R&D Systems), bovine serum albumin (BSA, Sigma) or poly-
97 L-lysine (Sigma). Wells were then exposed to a solution of 1mg/ml heat-denatured
98 BSA (Sigma) for 1 hr. Endometrial cells were trypsinised and incubated with various
99 concentrations of antibody (H-300-L rabbit anti-CD44 (Santa Cruz) or IgG from rabbit
100 serum as negative control, (Sigma); 5, 10 or 20µg/ml in serum-free medium (Teramoto
101 *et al.*, 2005) for 5 min at room temperature then plated into wells at 2000 cells/well.
102 Cells were cultured for 1 hr then imaged using phase contrast microscopy and
103 analysed using ImageJ.

104 *In-vitro attachment assay*

105 Confluent endometrial cells were incubated in serum-free medium (DMEM, 2mM
106 L-glutamine, 100µg/ml streptomycin and 100IU/ml penicillin) for 24 hrs prior to
107 co-culture with hatched E4.5 mouse blastocysts (3 per well), as previously described
108 (Ruane *et al.*, 2017).

109 In some experiments, medium was spiked with antibody (H-300-L rabbit anti-CD44 or
110 IgG from rabbit serum) at 20µg/ml (determined by data from the cell spreading
111 inhibition assay), either just prior to addition of E4.5 embryos or 24 hrs later just prior to
112 detachment of E5.5 embryos, by gently flushing with 60µl medium. Mouse embryos
113 flushed at day 4.5 require 28 hrs of incubation with cells to activate them for stable
114 attachment; flushing restored all embryos to an unattached state at the start of the

115 antibody incubation period. Other experiments involved pre-treatment of embryos and /
116 or Ishikawa cells with hyaluronidase prior to co-culture. Here hatched E4.5 blastocysts
117 were cultured in KSOM, 0.4% BSA to E5.5, then incubated with, or without, 500 IU/ml
118 hyaluronidase (Sigma) in KSOM, 0.4% BSA for 30 minutes before transfer onto treated
119 or untreated cells. Ishikawa cells were treated by culturing as usual for 24 hrs,
120 removing and retaining the conditioned medium during a 30 min incubation with 500
121 IU/ml hyaluronidase (in fresh serum-free culture medium), then replacing the retained
122 medium before adding treated or untreated E5.5 embryos.

123 In all experiments, attachment stability was assessed as previously described (Ruane
124 *et al.*, 2017), every 4 hrs during the first 12 hrs of co-culture then at 24, 28, 32, 36 hrs
125 and finally at 48 hrs (E6.5 of mouse embryo development) using an inverted phase
126 contrast microscope (Evos XL Core). Co-cultures were then fixed with 4% PFA for 20
127 min at room temperature and stored under PBS at 4°C.

128 *Single embryo fluorescence staining*

129 Hatched E4.5 embryos were fixed in a staining solution (3% BSA in PBS) containing
130 1% PFA for 20 min, quenched in 50mM ammonium chloride for 5 min, then
131 permeabilised using 0.5% Triton-X100 PBS solution for 6 min. Blastocysts were
132 incubated overnight at 4°C in a 25µl drop of staining solution containing H-300-L rabbit
133 anti-CD44 or IgG from rabbit serum under mineral oil (Sigma) followed by staining
134 solution containing an Alexa Fluor 488-labelled secondary antibody (Life
135 Technologies) and 4',6-diamidino-2-phenylindole (DAPI, Sigma) for 1 hr. Embryos
136 were mounted in a poly-L lysine-coated chamber of 3% 1,4-diazabicyclo[2.2.2]octane
137 (DABCO, Sigma) in PBS.

138 *Endometrial/endothelial cells and embryo attachment staining*

139 PFA-fixed cells and co-cultures were quenched with 50mM ammonium chloride before
140 permeabilisation in 0.5% Triton-X100 PBS. Mouse monoclonal anti-CD44 antibody
141 (5F12, NeoMarkers Fremont) and IgG from mouse serum (negative control, Sigma)
142 and Alexa Fluor 488-labelled secondary antibody (Life Technologies) were used to
143 stain Ishikawa cells and attachment sites. Rabbit polyclonal (H-300-L, Santa Cruz) was
144 used in some experiments. Hyaluronan was visualised by incubating samples for 3 hrs
145 at room temperature with a biotinylated hyaluronan binding protein (Biotin-HABP,
146 Amsbio), followed by streptavidin-fluorescein isothiocyanate for 1 hr at room
147 temperature. Nuclear and actin stains were performed using a mixture of DAPI (Sigma)
148 and Alexa Fluor® 568-coupled Phalloidin (Invitrogen). Coverslips with cell layers were
149 mounted upside down on a microscope slide in a drop of Mowiol 4-88 mounting
150 medium (Sigma) containing 3% DABCO. Coverslips with embryo-Ishikawa cells were
151 mounted a chamber of 3% DABCO in PBS to maintain the 3D structure of the
152 attachment sites.

153 *Fluorescence microscopy*

154 Fluorescence microscopy images were taken with an inverted Zeiss microscope, Zen
155 2.0 software and the Apotome 2 module, and analysed with ImageJ. Z-series optical
156 sections of cells were obtained at the minimum of 0.24µm increments for 40X and 63X
157 objectives. Z-stacks of embryo and embryo attachment sites were obtained at 1-2µm
158 increments at 40X for a maximal distance of 60µm.

159 *Statistics*

160 Data generated from embryo attachment assays and cell spreading assays are
161 represented as mean \pm the standard error of the mean or median and interquartile
162 range. Statistical analysis using Prism software (Graph-Pad, USA) included the 2-way

163 ANOVA test followed by Bonferroni's multiple comparisons post-hoc test or non-
164 parametric Wilcoxon, Mann-Whitney & Friedman tests.

165 **Results**

166 *CD44 immunoreactivity in blastocysts and Ishikawa cells*

167 The rabbit polyclonal antibody H300 against CD44 showed heterogeneous binding in
168 the trophectoderm of chemically hatched mouse blastocysts (Figure 1A-C). As
169 previously reported (Behzad *et al.*, 1994, Singh *et al.*, 2010), Ishikawa cells express
170 CD44. The monoclonal antibody 5F12, which did not show any reactivity with mouse
171 embryos, revealed linear lateral distribution of immunoreactivity as well as more diffuse
172 punctate staining in Ishikawa cells, with considerable intercellular variation (Figure 1D).
173 Heterogeneous immunoreactivity was in ruffles at the apical surface (Figure 1E).
174 Variation of culture conditions, including the presence and absence of serum and/or
175 matrigel as a substrate, did not cause significant changes (not shown).

176 *CD44 immunoreactivity in attachment sites in vitro*

177 Transfer of hatched E4.5 mouse blastocysts to Ishikawa epithelial cell monolayers is
178 followed by an initial period (28 hrs) of weak and reversible attachment that initiates
179 the activation required for embryos to progress, over the next 20 hrs, from stable
180 attachment to breaching and displacement of the underlying cells (Ruane *et al.*, 2017).
181 Figure 2A shows 5F12 reactivity in cells surrounding an attachment site with no
182 trophoblast invasion, whereas in Figure 2B, the trophoblast has breached the
183 subjacent cell layer and is beginning to laterally invade, with CD44-positive epithelial
184 cells crowded together in adjacent locations. Figure 2C surveys a subsequent stage in
185 which trophoblast giant cells with prominent stress fibres are apparent spreading over

186 the substrate. Intensity scans of such sites showed no significant change in CD44
187 immunoreactivity in cells adjacent to the embryo either at this or earlier pre-breaching
188 stages of attachment (not shown). Note this antibody does not detect staining in cells
189 in adherent embryos.

190 *Function-blocking antibody to CD44 can delay attachment*

191 To test the hypothesis that CD44 might mediate attachment of blastocysts to epithelial
192 cell layers, a function-blocking antibody, H300, was introduced into co-cultures. HA
193 does not bind to culture plastic, so the potency of H300 as an inhibitor of CD44
194 function in Ishikawa cells was examined using an adhesion assay which monitors the
195 capacity of cells to spread on dishes coated with OPN (Figure 3A,B). Inclusion of H300
196 resulted in partial inhibition (~ 55%) of spreading when cells were plated on OPN but
197 the antibody had no effect when a control substrate containing poly-L-lysine was used.

198 Alterations to embryo behaviour in response to antibody inhibition of CD44 function
199 were evaluated using a stability scale in which unattached and weakly attached
200 embryos can be reliably distinguished from those achieving intermediate or fully stable
201 attachment (Ruane *et al.*, 2017). Unattached embryos move across the monolayer
202 when disturbed, while weakly and intermediately attached embryos are identifiable by
203 high and low levels of oscillation, respectively, about an attachment point. Stably
204 attached embryos do not oscillate. Combining intermediate and stable attachment
205 scores produces a measure of irreversible attachment (Ruane *et al.*, 2017).

206 Introducing antibody to cultures just prior to the addition of E4.5 embryos impacted on
207 weak attachment in the first 8 hrs, and inhibited the level of stable attachment levels at
208 32 hrs co-culture (Figure 3C,D). In a second series of experiments, the antibody was
209 added after 24 hrs co-culture when embryos were at E5.5 and beginning to advance

210 from weak to stable attachment. Weakly adherent embryos were mechanically
211 detached at the time of antibody addition, which we have previously demonstrated
212 does not impact on their ability to progress to stable attachment (Ruane *et al.*, 2017).
213 Antibody spiking at this time point reduced total attachment levels between 28 and 32
214 hrs, though by 36 hrs the treated embryos had caught up with controls. Moreover, a
215 trend towards reduced stable attachment was observed from 28-36 hrs with significant
216 inhibition of stable attachment at 36 hrs (Figure 3E,F).

217 *A role for endometrial hyaluronan in early embryo attachment*

218 A fluorescent conjugate of the HA-binding domain of versican applied to fixed Ishikawa
219 cells revealed prominent fluorescence, demonstrating HA localisation at the apical
220 surface, where embryos initially dock (Figure 4A). After treatment with the enzyme
221 Hyal2, which cleaves high molecular mass HA into smaller fragments, cells showed a
222 negligible level of fluorescence (Figure 4B,C). There was no change in CD44
223 distribution in the treated cells (Figure 4D,E).

224 We then went on to investigate whether this apical surface-localised HA might
225 contribute to the attachment reaction. We carried out co-cultures from E5.5, using cells
226 and/or embryos pre-treated with Hyal2. Embryos stably attached more rapidly to cells
227 that had been treated with the enzyme, the difference being apparent between 28 and
228 32 hrs; by 48 hrs the embryos had attached as stably as in untreated controls (Figure
229 4F,G). Comparing total attachment levels with those of stable attachment
230 demonstrated that loss of HA has little effect on weak attachment at this embryonic
231 stage (Figure 4F,G). Treating embryos with Hyal2 had no effect on attachment kinetics
232 (Figure 4F,G).

233 **Discussion**

234 Our model system allows a detailed analysis of the kinetics of embryo attachment,
235 which progresses from a reversible weak stage, with activation of trophoblast gene
236 expression, to an irreversible stable stage that rapidly progresses to epithelial
237 breaching (Kang *et al.*, 2014, Ruane *et al.*, 2017). CD44 immunoreactivity in Ishikawa
238 cells and blastocysts is consistent with our previously reported analysis of the apical
239 Ishikawa glycoproteome (Singh and Aplin, 2015) and matches CD44 localisation in
240 human and murine blastocysts (Campbell *et al.*, 1995; Lu *et al.*, 2002). Data herein
241 reveal that the presence of a function-blocking CD44 antibody leads to a delay in the
242 progression of embryos to a stably attached state. Additionally, we found that
243 enzymatic degradation of the CD44 ligand HA from the apical surface of Ishikawa cell
244 layers, but not the blastocyst, hastened the attainment of stable attachment, with
245 minimal effects on weak attachment. Together these data suggest that CD44
246 contributes to weak embryo attachment in a HA-independent manner while
247 endometrial HA acts as a brake on progression to stable attachment.

248 Reflecting these data, pharmacological inhibition of uterine HA synthesis in sheep
249 leads to its disappearance from the uterine apical epithelial surface and a
250 corresponding increase in embryo attachment. Conversely, infusion of HA into the
251 lumen inhibits implantation (Marei *et al.*, 2017). HA may therefore act analogously to
252 the functions of mucins MUC1 and MUC16 (Aplin, 2000, Dharmaraj *et al.*, 2014,
253 Gipson *et al.*, 2008, Hey *et al.*, 1994, Meseguer *et al.*, 2001). Moreover, embryonic
254 activity causing loss of HA from the epithelial surface, as seen for MUC1 (Meseguer *et*
255 *al.*, 2001, Singh *et al.*, 2010), may underlie the progression to stable attachment.

256 The use of HA as a supplement at the time of embryo transfer has received
257 considerable attention in ART (Fouladi-Nashta *et al.*, 2017, Singh *et al.*, 2015), and

258 there is evidence to suggest that exogenous HA can bind to the luminal apical
259 epithelial cell membrane (Marei *et al.*, 2017). Supplementation would be justified only if
260 HA can be demonstrated to have a role in improving embryo viability, acquisition of
261 blastocyst adhesion competence or supporting development that precedes the
262 interaction with maternal epithelium at the start of implantation. Embryo development
263 and viability were found to be improved after culture in HA-supplemented media in
264 humans (Simon *et al.*, 2003) and in other animal models (Gardner *et al.*, 1999, Romek
265 *et al.*, 2017, Lane *et al.*, 2003). Exogenous HA may actually delay rather than promote
266 implantation in humans, and this impact on timing could underlie the beneficial effects
267 of such transfer medium by allowing acclimatisation of the blastocyst to the uterine
268 environment before implantation, or indeed synchronising a delayed window of
269 receptivity with the implantation-ready blastocyst. HA-enriched transfer medium has
270 also been shown to be beneficial during cleavage-stage embryo transfer (Urman *et al.*,
271 2008; Nakagawa *et al.*, 2012), implying that exogenous HA impacts upon embryo
272 development or the acquisition of a receptive endometrium. However, the beneficial
273 effect of HA-supplementation embryo transfer medium on implantation rate and clinical
274 pregnancy is controversial (Simon *et al.*, 2003, Fancsovits *et al.*, 2015).

275 The presence of CD44 at the blastocyst-uterine interface is not essential for
276 implantation in mice: CD44 null mice are fertile and viable with no morphological defect
277 (Schmits *et al.*, 1997, Protin *et al.*, 1999). In these studies, CD44 null offspring from
278 heterozygotic matings followed Mendelian rules, and their fertility status was reported,
279 though not shown, based on breeding of the F₁ generation. Another HA-binding
280 receptor, RHAMM, is expressed both in blastocysts (Choudhary *et al.*, 2009) and
281 endometrium (Rein *et al.*, 2003, Ozbilgin *et al.*, 2012), and could potentially
282 compensate for the absence of CD44 (Nedvetzki *et al.*, 2004, Naor *et al.*, 2007, Toole,

283 2009), but it has not been investigated in CD44-null animals. Further investigations are
284 necessary to determine the role of RHAMM in embryo attachment at implantation.

285 The anti-CD44 antibody we used has been shown to block binding of OPN to the N-
286 terminus (Teramoto *et al.*, 2005). Since this is also the major binding site in CD44 for
287 HA, the antibody is likely to impair HA binding (Banerji *et al.*, 2007, Peach *et al.*, 1993).
288 In the cell spreading assay, targeting CD44 was not expected to achieve a full
289 inhibition as the endometrial cells express integrins also known to interact with OPN
290 (Kang *et al.*, 2014). Furthermore, our HA clearance data suggest endogenous OPN is
291 the more likely ligand involved in CD44-mediated early attachment between
292 trophoderm and endometrial epithelial cells (Kang *et al.*, 2014). This study provides
293 evidence of a role for the CD44-OPN-HA axis in timely progression from weak
294 (CD44-OPN) to stable (loss of HA) attachment, which we believe is important for the
295 development of the invasive trophoblast required for the establishment of pregnancy
296 (Ruane *et al.*, 2017). If the observations were to translate to human embryos
297 implanting in vivo, a delay of a few hours towards the end of the receptive phase might
298 lead to failure to rescue the corpus luteum, and subsequent loss of the pregnancy
299 (Baird *et al.*, 1991). Conversely, rapid stable attachment caused by reduced HA could
300 allow the implantation of developmentally incompetent embryos with the potential to
301 miscarry (Aplin *et al.*, 1996, Quenby *et al.*, 2002, Teklenburg *et al.*, 2010).

302 In conclusion, our study demonstrates for the first time the role of CD44 at the early
303 stages of embryo-uterine attachment using an in-vitro implantation model and sets the
304 scene for further investigations to determine the role of other HA-receptors and CD44
305 ligands at implantation.

306 **Authors' roles**

307 S.C.B., S.J.K., M.W. and J.D.A. designed the study, and S.J.K., D.R.B., M.W. and J.D.A.
308 obtained funding. S.C.B. carried out the experimental work. J.D.A., S.C.B. and P.T.R.
309 wrote the paper, which was edited by S.J.K., D.R.B. and M.W.

310 **Funding**

311 This work was supported by funds from the charity Diabetes UK (15/0005207) and
312 studentship support for S.C.B. from the Anatomical Society.

313 **Conflict of interest**

314 None declared

315 **References**

316 Afify AM, Craig S, Paulino AF. Temporal variation in the distribution of hyaluronic acid,
317 CD44s, and CD44v6 in the human endometrium across the menstrual cycle. *Appl*
318 *Immunohistochem Mol Morphol* 2006;**14**:328-333.

319 Albers A, Thie M, Hohn HP, Denker HW. Differential expression and localization of
320 integrins and CD44 in the membrane domains of human uterine epithelial cells during
321 the menstrual cycle. *Acta Anat (Basel)* 1995;**153**:12-19.

322 Aplin JD. The cell biological basis of human implantation. *Baillieres Best Pract Res*
323 *Clin Obstet Gynaecol* 2000;**14**:757-764. Aplin JD. The cell biological basis of human
324 implantation. *Baillieres Best Pract Res Clin Obstet Gynaecol* 2000;**14**:757-764.

325 Aplin JD, Hey NA, Li TC. MUC1 as a cell surface and secretory component of
326 endometrial epithelium: reduced levels in recurrent miscarriage. *Am J Reprod*
327 *Immunol* 1996;**35**:261-266.

- 328 Aplin JD, Ruane PT. Embryo-epithelium interactions during implantation at a glance. *J*
329 *Cell Sci* 2017;**130**:15-22.
- 330 Baird DD, Weinberg CR, Wilcox AJ, McConnaughey DR, Musey PI, Collins DC.
331 Hormonal profiles of natural conception cycles ending in early, unrecognized
332 pregnancy loss. *J Clin Endocrinol Metab* 1991;**72**:793-800.
- 333 Banerji S, Wright AJ, Noble M, Mahoney DJ, Campbell ID, Day AJ, Jackson DG.
334 Structures of the Cd44-hyaluronan complex provide insight into a fundamental
335 carbohydrate-protein interaction. *Nat Struct Mol Biol* 2007;**14**:234-239.
- 336 Behzad F, Seif MW, Campbell S, Aplin JD. Expression of two isoforms of CD44 in
337 human endometrium. *Biol Reprod* 1994;**51**:739-747.
- 338 Bontekoe S, Heineman MJ, Johnson N, Blake D. Adherence compounds in embryo
339 transfer media for assisted reproductive technologies. *Cochrane Database Syst Rev*
340 2014;**2**:CD007421.
- 341 Campbell S, Swann HR, Aplin JD, Seif MW, Kimber SJ, Elstein M. CD44 is expressed
342 throughout pre-implantation human embryo development. *Hum Reprod* 1995;**10**:425-
343 430.
- 344 Choudhary M, Zhang X, Stojkovic P, Hyslop L, Anyfantis G, Herbert M, Murdoch AP,
345 Stojkovic M, Lako M. Putative role of hyaluronan and its related genes, HAS2 and
346 RHAMM, in human early preimplantation embryogenesis and embryonic stem cell
347 characterization. *Stem Cells* 2007;**25**:3045-57.

- 348 Dharmaraj N, Chapela PJ, Morgado M, Hawkins SM, Lessey BA, Young SL, Carson
349 DD. Expression of the transmembrane mucins, MUC1, MUC4 and MUC16, in normal
350 endometrium and in endometriosis. *Hum Reprod* 2014;**29**:1730-1738.
- 351 Fancsovits P, Lehner A, Murber A, Kaszas Z, Rigo J, Urbancsek J. Effect of
352 hyaluronan-enriched embryo transfer medium on IVF outcome: a prospective
353 randomized clinical trial. *Arch Gynecol Obstet* 2015;**291**:1173-9.
- 354 Fouladi-Nashta AA, Raheem KA, Marei WF, Ghafari F, Hartshorne GM. Regulation
355 and roles of the hyaluronan system in mammalian reproduction. *Reproduction*
356 2017;**153**:R43-R58.
- 357 Fujita N, Yaegashi N, Ide Y, Sato S, Nakamura M, Ishiwata I, Yajima A. Expression of
358 CD44 in normal human versus tumor endometrial tissues: possible implication of
359 reduced expression of CD44 in lymph-vascular space involvement of cancer cells.
360 *Cancer Res* 1994;**54**:3922-3928.
- 361 Gardner DK, Rodriegez-Martinez H, Lane M. Fetal development after transfer is
362 increased by replacing protein with the glycosaminoglycan hyaluronan for mouse
363 embryo culture and transfer. *Hum Reprod* 1999;**14**:2575-80.
- 364 Gipson IK, Blalock T, Tisdale A, Spurr-Michaud S, Allcorn S, Stavreus-Evers A,
365 Gemzell K. MUC16 is lost from the uterodome (pinopode) surface of the receptive
366 human endometrium: in vitro evidence that MUC16 is a barrier to trophoblast
367 adherence. *Biol Reprod* 2008;**78**:134-142.
- 368 Griffith JS, Liu YG, Tekmal RR, Binkley PA, Holden AE, Schenken RS. Menstrual
369 endometrial cells from women with endometriosis demonstrate increased adherence

- 370 to peritoneal cells and increased expression of CD44 splice variants. *Fertil Steril*
371 2010;**93**:1745-1749.
- 372 Goldsmith HL, Labrosse JM, McIntosh FA, Mäenpää PH, Kaartinen MT, McKee MD.
373 Homotypic interactions of soluble and immobilized osteopontin. *Ann Biomed Eng*
374 2002;**30**:840-50.
- 375 Hey NA, Graham RA, Seif MW, Aplin JD. The polymorphic epithelial mucin MUC1 in
376 human endometrium is regulated with maximal expression in the implantation phase.
377 *J Clin Endocrinol Metab* 1994;**78**:337-342.
- 378 Johnson GA, Burghardt RC, Bazer FW. Osteopontin: a leading candidate adhesion
379 molecule for implantation in pigs and sheep. *J Anim Sci Biotechnol* 2014;**5**:56.
- 380 Kang YJ, Forbes K, Carver J, Aplin JD. The role of the osteopontin-integrin
381 alphavbeta3 interaction at implantation: functional analysis using three different in vitro
382 models. *Hum Reprod* 2014;**29**:739-749.
- 383 Lane M, Maybach JM, Hooper K, Hasler JF, Gardner DK. Cryo-survival and
384 development of bovine blastocysts are enhanced by culture with recombinant albumin
385 and hyaluronan. *Mol Reprod Dev* 2003;**64**:70-78.
- 386 Lu DP, Tian L, O'Neill C, King NJ. Regulation of cellular adhesion molecule
387 expression in murine oocytes, peri-implantation and post-implantation embryos. *Cell*
388 *Res* 2002;**12**:373-383.
- 389 Marei WFA, Wathes DC, Raheem KA, Mohey-Elsaeed O, Ghafari F, Fouladi-Nashta
390 AA. Influence of hyaluronan on endometrial receptivity and embryo attachment in
391 sheep. *Reprod Fertil Dev* 2017;**29**:1763-1773.

- 392 Meseguer M, Aplin JD, Caballero-Campo P, O'Connor JE, Martin JC, Remohi J,
393 Pellicer A, Simon C. Human endometrial mucin MUC1 is up-regulated by
394 progesterone and down-regulated in vitro by the human blastocyst. *Biol Reprod*
395 2001;**64**:590-601.
- 396 Misra S, Hascall VC, Markwald RR, Ghatak S. Interactions between Hyaluronan and
397 Its Receptors (CD44, RHAMM) Regulate the Activities of Inflammation and Cancer.
398 *Front Immunol* 2015;**6**:201.
- 399 Mohamed OA, Jonnaert M, Labelle-Dumais C, Kuroda K, Clarke HJ, Dufort D. Uterine
400 Wnt/beta-catenin signaling is required for implantation. *Proc Natl Acad Sci U S A*
401 2005;**102**:8579-8584.
- 402 Nakagawa K, Takahashi C, Nishi Y, Jyuen H, Sugiyama R, Kuribayashi Y, Sugiyama
403 R. Hyaluronan-enriched transfer medium improves outcome in patients with multiple
404 embryo transfer failures. *J Assist Reprod Genet* 2002;**29**:679-85.
- 405 Noar D, Nedvetszki S, Walmsley M, Yayon A, Turley EA, Golan I, Caspi D, Sebban
406 LE, Zicky Y, Garin T *et al.* CD44 involvement in autoimmune inflammations: the
407 lesson to be learned from CD44-targeting by antibody or from knockout mice. *Ann N Y*
408 *Acad Sci* 2007;**1110**:233-47.
- 409 Nedvetszki S, Gonen E, Assayag N, Reich R, Williams RO, Thurmond RL, Huang JF,
410 Neudecker BA, Wang FS, Turley EA *et al.* RHAMM, a receptor for hyaluronan-
411 mediated motility, compensates for CD44 in inflamed CD44-knockout mice: a different
412 interpretation of redundancy. *Proc Natl Acad Sci U S A* 2004;**101**:18081-18086.

- 413 Ozbilgin K, Boz B, Tuğyan K, Inan S, Vatansever S. RHAMM expression in the rat
414 endometrium during the estrous cycle and following implantation. *J Reprod Infertil*
415 2012;**13**:131-7.
- 416 Peach RJ, Hollenbaugh D, Stamenkovic I, Aruffo A. Identification of hyaluronic acid
417 binding sites in the extracellular domain of CD44. *J Cell Biol* 1993;**122**:257-264.
- 418 Protin U, Schweighoffer T, Jochum W, Hilberg F. CD44-deficient mice develop
419 normally with changes in subpopulations and recirculation of lymphocyte subsets. *J*
420 *Immunol* 1999;**163**:4917-23.
- 421 Quenby S, Vince G, Farquharson R, Aplin J. Recurrent miscarriage: a defect in
422 nature's quality control? *Hum Reprod* 2002;**17**:1959-1963.
- 423 Rein DT, Roehrig K, Schöndorf T, Lazar A, Fleisch M, Niederacher D, Bender HG,
424 Dall P. Expression of the hyaluronan receptor RHAMM in endometrial carcinomas
425 suggests a role in tumour progression and metastasis. *J Cancer Res Clin Oncol*
426 2003;**129**:161-4.
- 427 Romek M, Gajba B, Krzysztofowicz E, Kucia M, Uzarowska A, Smorag Z. Improved
428 quality of porcine embryos cultured with hyaluronan due to the modification of the
429 mitochondrial membrane potential and reactive oxygen species level. *Theriogenology*
430 2017;**102**:1-9.
- 431 Ruane PT, Berneau SC, Koeck R, Watts J, Kimber SJ, Brison DR, Westwood M, Aplin
432 JD. Apposition to endometrial epithelial cells activates mouse blastocysts for
433 implantation. *Mol Hum Reprod* 2017;**23**:617-627.

- 434 Ruane PT, Koeck R, Berneau SC, Kimber SJ, Westwood M, Brison DR, Aplin JD.
435 Osmotic stress induces JNK-dependent embryo invasion in a model of implantation.
436 *Reproduction* 2018;**156**:421-428.
- 437 Saegusa M, Hashimura M, Okayasu I. CD44 expression in normal, hyperplastic, and
438 malignant endometrium. *J Pathol* 1998;**184**:297-306.
- 439 Saegusa M, Okayasu I. Up-regulation of CD44 variant exon expression in endometrial
440 carcinomas: analysis of mRNA and protein isoforms, and relation to
441 clinicopathological factors. *Jpn J Cancer Res* 1998;**89**:291-298.
- 442 Schmits R, Filmus J, Gerwin N, Senaldi G, Kiefer F, Kundig T, Wakeham A, Shahinian
443 A, Catzavelos C, Rak J *et al.* CD44 regulates hematopoietic progenitor distribution,
444 granuloma formation, and tumorigenicity. *Blood* 1997;**90**:2217-2233.
- 445 Senbanjo LT, Chellaiah MA. CD44: A Multifunctional Cell Surface Adhesion Receptor
446 Is a Regulator of Progression and Metastasis of Cancer Cells. *Front Cell Dev Biol*
447 2017;**5**:18.
- 448 Simon A, Safran A, Revel A, Aizenman E, Reubinoff B, Porat-Katz A, Lewin A, Laufter
449 N. Hyaluronic acid can successfully replace albumin as the sole macromolecule in a
450 human embryo transfer medium. *Fertil Steril* 2003;**79**:1434-1438.
- 451 Singh H, Aplin JD. Endometrial apical glycoproteomic analysis reveals roles for
452 cadherin 6, desmoglein-2 and plexin b2 in epithelial integrity. *Mol Hum Reprod*
453 2015;**21**:81-94.

454 Singh N, Gupta M, Kriplani A, Vanamail P. Role of Embryo Glue as a transfer medium
455 in the outcome of fresh non-donor in-vitro fertilization cycles. *J Hum Reprod Sci*
456 2015;**8**:214-217.

457 Singh H, Nardo L, Kimber SJ, Aplin JD. Early stages of implantation as revealed by an
458 in vitro model. *Reproduction* 2010;**139**:905-914.

459 Teklenburg G, Salker M, Heijnen C, Macklon NS, Brosens JJ. The molecular basis of
460 recurrent pregnancy loss: impaired natural embryo selection. *Mol Hum Reprod*
461 2010;**16**:886-895.

462 Teramoto H, Castellone MD, Malek RL, Letwin N, Frank B, Gutkind JS, Lee NH.
463 Autocrine activation of an osteopontin-CD44-Rac pathway enhances invasion and
464 transformation by H-RasV12. *Oncogene* 2005;**24**:489-501.

465 Toole BP. Hyaluronan-CD44 interactions in cancer: paradoxes and possibilities. *Clin*
466 *Cancer Res* 2009;**15**:7462-7468.

467 Urman B, Yakin K, Ata B, Isiklar A, Balaban B. Effect of hyaluronan-enriched transfer
468 medium on implantation and pregnancy rates after day 3 and day 5 embryo transfers:
469 a prospective randomized study. *Fertil Steril* 2008;**90**:604-12.

470 Zheng Q, Zhang D, Yang YU, Cui X, Sun J, Liang C, Qin H, Yang X, Liu S, Yan Q.
471 MicroRNA-200c impairs uterine receptivity formation by targeting FUT4 and alpha1,3-
472 fucosylation. *Cell Death Differ* 2017;**24**:2161-2172.

473 **Figure legends**

474 **Figure 1 CD44 in embryos and Ishikawa cells.** **A, B.** An E4.5 mouse blastocyst
475 fixed in PFA and stained for CD44 using polyclonal antibody H-300 (green). The

476 embryo is represented using a single Z-plane of the Z-stack together with a X-Z plane
477 image below the blue line from the point indicated by the arrow (A) or in 3D (B). **C.**
478 Rabbit serum IgG is a negative control. Blue: cell nuclei (DAPI). 5 embryos were
479 stained in 2 batches. **D, E.** Representative fluorescence images of localisation of
480 CD44 (green) at Ishikawa cell lateral membranes using monoclonal antibody 5H12 in
481 the mid-plane (D) or apical plane (E). The actin cytoskeleton is red (Alexafluor 594-
482 phalloidin). The X-Z plane (bottom of image) reveals CD44-positive epithelium. N=3.
483 **F.** Negative control (anti-KLH monoclonal with rhodamine-phalloidin and DAPI). Scale
484 bar (B, C, F) = 20 μ m.

485 **Figure 2 CD44 in embryo-epithelial attachment sites.** Mouse embryos attached
486 after 48 hrs co-culture with Ishikawa cells were fixed and stained with antibody 5H12
487 (green), which detects human but not mouse CD44. **A.** The main image shows
488 confluent unbreached epithelial cells. An attached embryo is centred at the position of
489 the asterisk. The X-Z plane (bottom of image) collected on the line of the arrow
490 reveals trophoblast (arrow) attached to CD44-positive epithelium. **B.** A later stage in
491 which trophoblast has displaced epithelial cells. The area lacking green staining at
492 centre reveals the position of the embryo. A blue arrow again indicates the location of
493 the X-Z section shown at bottom, with white arrows indicating the embryonic periphery
494 where trophoblast and displaced epithelium are in apposition. **C.** Still later, with
495 prominent actin bundles (arrows in top left image) characteristic of trophoblast giant
496 cells in the plane of the substrate. The position of the embryo is also revealed by the
497 absence of CD44 staining in an area left of centre. Scale bars in A, B & C, 50 μ m.

498 **Figure 3 Characterisation of impact of anti-CD44 antibody on embryo**
499 **attachment and stability.** **A, B.** Ishikawa cell spreading assay in which trypsinised

500 cells were plated on the indicated substrates and incubated for 1 hr. Spreading was
501 scored with the aid of a phase contrast microscope. Control cells spread on culture
502 plastic, poly-lysine, or osteopontin. The anti-CD44 polyclonal antibody H300 effects
503 partial inhibition of spreading on osteopontin but does not influence behaviour on the
504 other substrates. **C, D.** Embryo-epithelial attachment assay with H-300 antibody
505 added just prior to co-culture from E4.5. Three conditions, control (no antibody),
506 anti-CD44 antibody and control IgG, are respectively represented in blue, red and
507 green. All conditions were analysed for the percentage of embryos attached either
508 weakly, intermediately or stably, and those that had advanced to attach intermediately
509 and stably. **E, F.** Plots show attachment when antibody was added to detached
510 embryo co-cultures after 24h. Data are presented as mean \pm SEM and statistical
511 analysis was performed using 2-way ANOVA with Bonferroni's multiple comparison
512 test (*: $P < 0.05$; **: $P < 0.01$; ****: $P < 0.001$). $N=4$ (48 embryos per condition).

513 **Figure 4 Effect of hyaluronidase treatment on embryo attachment.** **A.** The
514 HA-binding domain of versican (green) was used to reveal HA at the surface of
515 Ishikawa cell layers. The inset shows staining in the absence of binding protein. **B.**
516 After treatment with Hyal2, staining is lost. **C.** Quantification of HA fluorescence. **D.**
517 CD44 staining (green) before and after Hyal2 treatment of Ishikawa cells. Total green
518 fluorescent pixels above background before and after treatment, showing no
519 difference. Actin, red; DNA, blue. Scale bars in A, B & D, 50 μ m. **E.** Quantification of
520 CD44 fluorescence. **F.** Mouse embryo total attachment from E5.5-6.5 under four
521 conditions of Hyal2 treatment of: embryos (red), Ishikawa cells (green), both (purple)
522 or neither (blue). **G.** Mouse embryo stable attachment plotted. Data are presented as
523 mean \pm SEM and statistical analysis was performed using 2-way ANOVA with

524 Bonferroni's multiple comparison test (*: $P < 0.05$; **: $P < 0.01$; ****: $P < 0.001$). N=4 (48
525 embryos per condition). Scale bar (A, B, D) = $50\mu\text{m}$

Figure 1

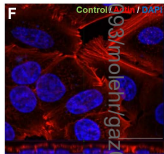
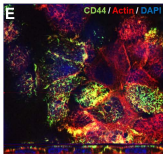
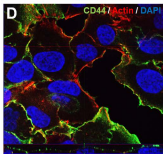
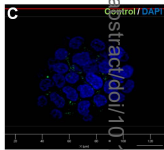
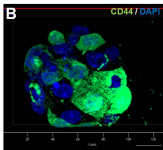
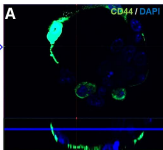


Figure 2

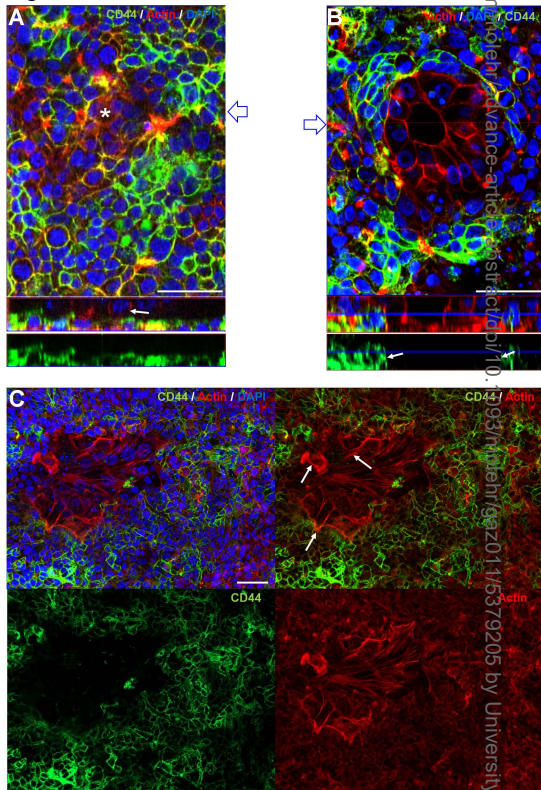
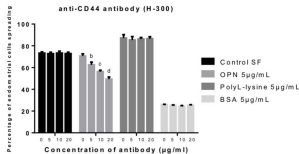
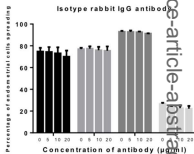


Figure 3

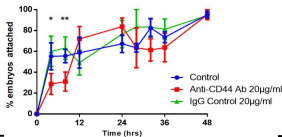
A



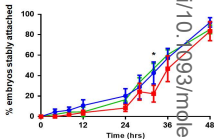
B



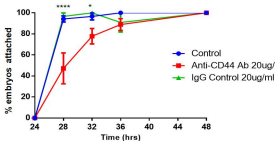
C



D



E



F

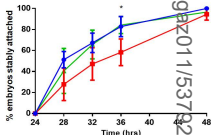


Figure 4

